

# A Locomotion Recognition System Using Depth Images

Tingfang Yan<sup>1</sup>, Yuxiang Sun<sup>1</sup>, Tingting Liu<sup>1</sup>, Chi-Hong Cheung<sup>2</sup>, Max Qing-Hu Meng<sup>\*1</sup>

**Abstract**—Powered lower-limb orthoses and prostheses are attracting an increasing amount of attention in assisting daily living activities. To safely and naturally collaborate with human users, the key technology relies on an intelligent controller to accurately decode users' movement intention. In this work, we proposed an innovative locomotion recognition system based on depth images. Composed of a feature extraction subsystem and a finite-state-machine based recognition subsystem, the proposed approach is capable of capturing both the limb movements and the terrains right in front of the user. This makes it possible to anticipate the detection of locomotion modes, especially at transition states, thus enabling the associated wearable robot to deliver a smooth and seamless assistance. Validation experiments were implemented with nine subjects to trace a track that comprised of standing, walking, stair ascending, and stair descending, for three rounds each. The results showed that in steady state, the proposed system could recognize all four locomotion tasks with approximate 100% of accuracy. Out of 216 mode transitions, 82.4% of the intended locomotion tasks can be detected before the transition happened. Thanks to its high accuracy and promising prediction performance, the proposed locomotion recognition system is expected to significantly improve the safety as well as the effectiveness of a lower-limb assistive device.

## I. INTRODUCTION

In recent years, the advancement of powered lower-limb wearable robots is gaining increasing attention [1], [2]. They are considered to be a novel active assistive and rehabilitation technology for those who have gait disorders [3], weakened mobility [4], [5], or even loss of locomotion functionality [6], [7]. Given a close human interaction, the wearable robots are designed to act compliantly and consistently with users' natural movements [8]. For the purpose of assisting users with their daily living activities, the wearable robot should be encoded with a skilled and delay-free controller that could accurately decode wearers' locomotion intention. Particularly, a prediction of the locomotion modes is of significance to ensure seamless and smooth assistive actions [9].

A number of strategies with various sensory systems have been developed in the state of the art [10]. One widely adopted approach is detecting the locomotion modes with surface electromyography (sEMG). Promising results with 95% of recognition accuracy have been reported by an active prosthesis when assisting amputees' locomotion [11]. However, the sEMG-based solution is limited by its low

<sup>1</sup>Department of Electronic Engineering, The Chinese University of Hong Kong, Shatin, N.T., Hong Kong. tfyan@ee.cuhk.edu.hk, yxsun@ee.cuhk.edu.hk, ttliu@ee.cuhk.edu.hk, max.meng@cuhk.edu.hk

<sup>2</sup>Division of Engineering Science, Faculty of Applied Science & Engineering, University of Toronto, Toronto, Canada. chihong.cheung@mail.utoronto.ca

\* corresponding author

accuracy in detecting mode transitions and its mandatory calibration procedure for each user. Furthermore, its performance can also be easily affected by the placement position of electrodes and skin temperature. In [6], a brain-machine interface based on measuring electroencephalogram (EEG) activities is proposed to control lower-limb exoskeletons in assisting the movements of people with paraplegia. Nevertheless, the difficulty of acquiring clean and stable EEG signals limits its range of applications. Locomotion detection based on mechanical sensors is another commonly adopted strategy. The most commonly used sensory systems include accelerometer, gyroscope [12], [13], pressure sensors [14], or a combination of different sensors [15]. The detection accuracy is quite promising, being 98.8% in [14]. Despite of the high accuracy, a delay is intrinsically involved in the transition detections. This is because each detection happens only after a critical feature of biomechanical signals is detected, for instance, foot placement.

Inspired by the motion control strategy of humans and animals, a subject-independent and environmental-aware strategy has been recently conceived for locomotion recognition. Seeing the terrain conditions in front the user could reinforce the decision-making of a locomotion mode recognition system and enable a seamless conversion of assistance delivery. A laser and IMU based sensory system is constructed in [16] to detect the terrain conditions, thus recognizing users' locomotion tendency. The classification method is a two-layer decision tree. In the first layer, the terrain is roughly divided into upper terrain, level ground and lower terrain. The uneven terrains are further recognized as ramp or stair in the second layer. The thresholds used in this work are taken from literature, which is not adaptive to the complicated real-life environments. In addition, the angle between the laser and the stairs should be aligned. Then, to close the loop of user and environment, the authors of [17] used depth sensing technology to segment and recognize stairs. Their system is capable to estimate the intersection angle and distance between the RGB-Depth camera and stairs, the number of steps, and the stair height and depth. The stair detection accuracy is greater than 98% in different environment conditions. But this system is only validated with upstairs segmentation. In [18], five different locomotion modes are detected with a depth camera mounted on the shank of one limb. The decision is made based on a support vector machine (SVM). This means that the detection accuracy will be affected by the sample size of training data for the SVM. Then, the camera mounted on the shank would bring huge variations and noises to the depth images, which will increase the difficulty of achieving an accurate detection.

The objective of this study is to design and validate an innovative locomotion mode recognition method by means of depth images. The proposed system is capable of: i) detecting different locomotion tasks with high accuracy, including standing, ground-level walking, and stair climbing; ii) during mode transition states, identifying the intended locomotion before the transition is completed; iii) carrying out locomotion recognition without pre-training; iv) being adaptive and robust to different users. For the sake of validating the prediction performance and detection accuracy of the proposed system, experiments have been implemented with nine subjects.

A detailed description of the depth image-based locomotion recognition system is presented in Section II. The validation experiments and results are discussed in Section III and Section IV respectively. At the end of the work, conclusions and future work are drawn in Section V.

## II. LOCOMOTION MODE RECOGNITION SYSTEM

A depth image-based locomotion mode recognition system is proposed in this study. The system consists of two subsystems: depth feature extraction and locomotion mode recognition. Before the detailed explanations of each subsystem, a brief overview of the setup for acquiring depth images is described at the beginning of this section.

### A. Depth Image Acquisition

In this study, the depth images are captured by Xtion PRO LIVE camera (ASUS), as shown in Fig. 1(a). The camera runs at 30 Hz and outputs depth images with a resolution of 640x480. Based on infrared sensors, the depth camera is capable to accurately estimating a distance between 0.8 m and 3.5 m. Its field of view angles are 58, 45 and 70 degrees in the horizontal, vertical, and diagonal directions, respectively. Fig. 1(b) illustrates the view field:  $HcOH$  represents the maximum horizontal view angle,  $HcOV$  represents the maximum vertical view angle, and  $HcOD$  represents the maximum diagonal view angle.

For the purpose of predicting the locomotion modes and identifying gait phase, we propose to fix the camera in front of users waist by means of a belt. The direction of the camera is tuned in a way that only a small portion of the user's feet is seen by the camera when the user is standing upright. As demonstrated in Fig. 1(c), when the camera is placed at the center of user's waist at  $Hc = 106$  cm, it could provide the depth values in the field highlighted by the red square. The distance from the toe to the edge of the view field is around 72 cm, which is within 1 stride length of walking [19].

### B. Depth Feature Extraction

To conceive an accurate locomotion detection system without introducing a heavy computation workload, we propose to extract two features: the local average depth values and stair edges. The first feature is used to obtain an initial locomotion mode classification while the second feature is expected to further improve the accuracy of the recognition. Details of each feature extraction are presented in the following text.

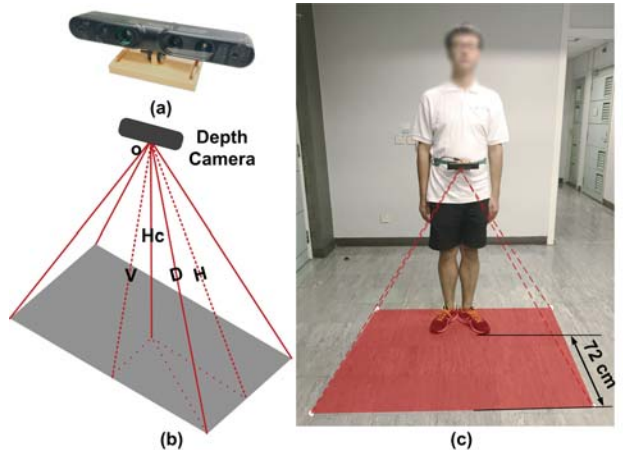


Fig. 1. Overview of the system setup for acquiring the depth images: (a) Xtion Pro Live camera; (b) The field of view angles of the depth camera: O is the position of the camera, Hc is the height of the camera regarding to the view plane, V, D, and H are vectors in the horizontal, vertical, and diagonal directions respectively; (c) Placement of the depth camera and its view field in standing still mode.

*1) Local average depth values:* Examples of the depth images captured during standing still (SS), ground level walking (GLW), stair ascending (SA), and stair descending (SD) modes are provided in Fig. 2. The darker colour is related to a smaller distance. When the distance is smaller than the view range of the camera (0.8 m), the depth value is 0. The example in Fig. 2 shows that in SA mode, the depth value at the top of the image is the smallest while in SD mode, it is the biggest. Although the top part the depth images in SS and GLW modes are quite similar, the two modes could be distinguished by referring to the bottom part of the image. When subject is walking on a level ground, the depth values at the bottom of the image change periodically because of the lower-limb movements.

Hence, we propose to divide the whole image into small blocks and then compute their depth values. In this study, the image is segmented into 3 rows and 4 columns, resulting in 12 blocks, as displayed in Fig. 3. The mean and standard deviations of each depth block are calculated and labelled as  $M_{i,j}$  and  $STD_{i,j}$  for the block in the  $i$ -th row  $j$ -th column, respectively.

*2) Stair Edge Detection:* As shown in Fig. 2, when the user is proceeding forward, there could be walls, handrails or other obstacles entering the camera's view and causing depth variations. In order to distinguish whether the variation is caused by locomotion transitions or obstacles, we propose to detect the stair edges by means of the Hough Line Transform [20].

Generally, a straight line in the Cartesian coordinates can be represented by two parameters, slope  $a$  and intercept  $b$ . The line equation is formed as follows:

$$y = a \cdot x + b \quad (1)$$

However, when the slope  $a$  approaches infinity, it is difficult to describe the straight line clearly with (1). Thus,

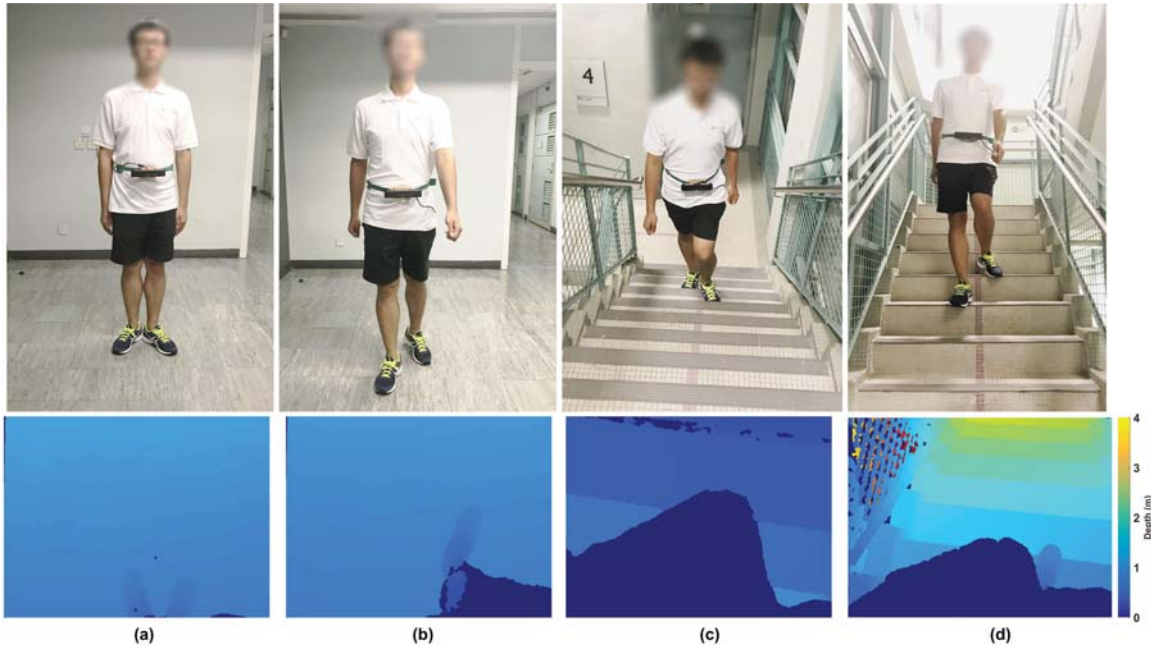


Fig. 2. Examples of the depth images captured in different locomotion modes. The four images in the second row are the depth images captured in (a) standing still mode, (b) level ground mode, (c) stair ascending mode, and (d) stair descending mode. The color gradient from dark blue to light yellow corresponds to a distance from 0 to 4 m.

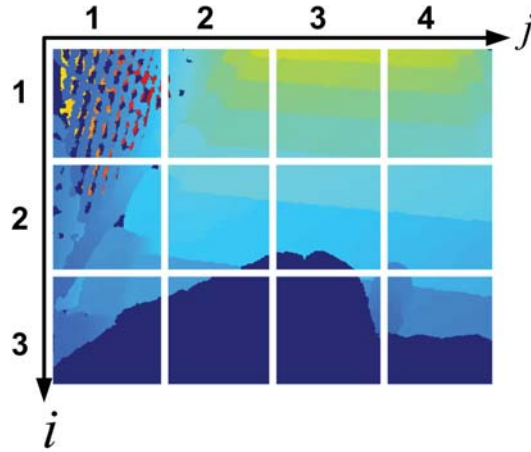


Fig. 3. Each depth image is divided into 12 blocks, having 3 rows and 4 columns.

it is proposed to convert the line parameterization to Polar coordinates(see Fig. 4(a)):

$$\rho = x \cdot \cos \theta + y \cdot \sin \theta \quad (2)$$

where  $\rho$  is the perpendicular distance from the origin to the straight line and  $\theta$  is angle of  $\rho$  measured in degrees clockwise from the positive  $x$ -axis. The range of  $\theta$  is  $-90^\circ \leq \theta \leq 90^\circ$ . The Hough Line Transform algorithm can be implemented directly with MATLAB or OpenCV functions. Thus, we will not repeat the details here. Fig. 4(b) has presented an example of the detected stair edges in a depth image. The approach is realized in MATLAB with a list of functions, including *edge()*, *hough()*, *houghpeaks()*, and

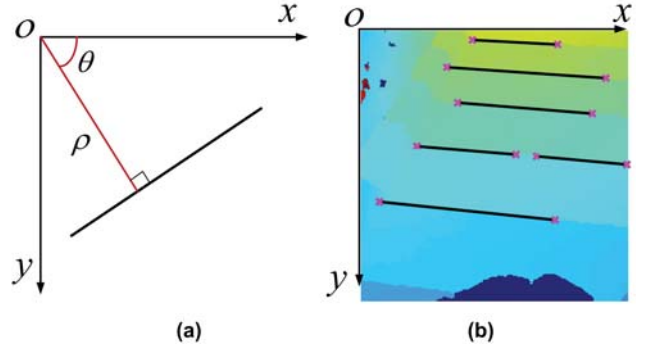


Fig. 4. Stair edge detection by means of Hough Line Transform: (a) line parameterization in Hough Transform, (b) the black straight lines are the detected stair edges in a depth image, and the magenta points indicate the end points of each line.

*houghlines()*. The final outputs are  $\theta$ ,  $\rho$ , and the end points positions of each line. When  $|\theta| > 65^\circ$  and the difference of depth values at the two sides of the line is greater than 0.1 m, the detected straight line is considered to be a stair edge.

### C. Locomotion Mode Detection

A finite state machine is designed to manage the detections and transitions of the four locomotion tasks: SS, GLW, SA, and SD. The task labels and transition conditions among tasks are shown in Fig. 5 and TABLE I respectively. In Fig. 5, the locomotion tasks are distinguished between static tasks, which include SS, and dynamic tasks, which include GLW, SA, and SD. To filter initial noises, two sliding windows are added on the top of the static task and dynamic task detection. The window sizes are 50 samples and 5 samples respectively.

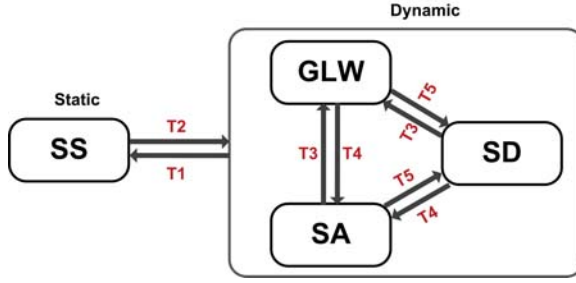


Fig. 5. Finite state machine for the locomotion detection system: T1, T2, T3, T4, and T5 are task labels for standing still, dynamic tasks, ground level walking, stair ascending, and stair descending, respectively.

According to the field of view graph displayed in Fig. 1, the depth camera has quite a big horizontal view, which will bring some noise to the depth image. In other words, the block depth values of the first and fourth columns may also vary due to obstacles entering the camera's view. To avoid these disturbances, only depth blocks of second and third columns, which mainly capture the terrain information and limb movements, are utilized to determine task transitions. Considering that the top two blocks, Block(1,2) and Block(1,3), represent the maximum view distance of the camera, we use them to estimate the terrain condition in front the user, thus enabling a prediction of the user's locomotion task. Block(3,2) and Block(3,3) always capture user's limbs and feet, so it is difficult to detect a stair edge in these two blocks. Therefore, instead of detecting stair edges in a whole depth image, the stair edge extraction only take part of the image. Here, the input image for stair edge extraction consists of four blocks: Block(1,2), Block(1,3), Block(2,2), and Block(2,3).

In TABLE I, the thresholds in T1,  $Th_{ss1}$  and  $Th_{ss2}$ , are set to be 0.02 m and 0.1 m respectively. Both values are selected by referring to the maximum standard deviations in the corresponding depth blocks in SS mode. As a result of the user's feet in Block(3,2),  $Th_{ss1}$  is smaller than  $Th_{ss2}$ . The thresholds  $Th_{sa1,j}$  and  $Th_{sd1,j}$  are calculated as follows:

$$Th_{sa1,j} = M_{ss1,j} - 3 * STD_{ss1,j} - H_{stair} \quad (3)$$

$$Th_{sd1,j} = M_{ss1,j} + 3 * STD_{ss1,j} + H_{stair} \quad (4)$$

where  $M_{ss1,j}$  and  $STD_{ss1,j}$  are the mean and standard deviations of corresponding depth blocks in SS mode respectively.  $H_{stair}$  is the height of each stair.

### III. EXPERIMENTS

#### A. Experimental Protocol

This experiment aimed to validate the accuracy of the depth image-based locomotion mode recognition system. Particularly, the timing of task transition detection was evaluated. The experimental setup was as presented in Sub-section II-A and Fig. 1(c).

Nine healthy young subjects (4 female and 5 male, height  $171 \pm 9.5$  cm, age  $25.2 \pm 1.2$  yrs) were recruited. Each subject was asked to follow a set path continuously three

TABLE I  
TRANSITION CONDITIONS AMONG THE LOCOMOTION TASKS

Task Label	Transition Conditions
T1	$STD_{2,2} < Th_{ss1} \wedge STD_{2,3} < Th_{ss1} \wedge STD_{3,2} < Th_{ss2}$ $\wedge STD_{3,3} < Th_{ss2}$
T2	NOT T1
T3	$Th_{sa1,2} < M_{1,2} < Th_{sd1,2} \vee Th_{sa1,3} < M_{1,3} < Th_{sd1,3}$ $\wedge$ No Stair Edge
T4	$M_{1,2} \leq Th_{sa1,2} \wedge M_{1,3} \leq Th_{sa1,3}$ $\wedge$ Stair Edge
T5	$M_{1,2} \geq Th_{sd1,2} \wedge M_{1,3} \geq Th_{sd1,3}$ $\wedge$ Stair Edge

times at his/her preferred speed. Each track was composed of 10 seconds of SS, then GLW, SA, GLW to turn 90 degrees, SA, GLW to turn 180 degrees, SD, GLW to turn 90 degrees, SD, GLW, and finally 10 seconds of SS. Thus each trace test covered transitions between SS and GLW, between GLW and SA, and between GLW and SD. All depth images were captured at a frequency of 30 Hz and saved for offline recognition and data analysis with MATLAB R2016a.

#### B. Data Analysis

The recognition performance was evaluated using two indexes: the recognition accuracy (RA) during steady state and the timing of transition detection. RA was defined as follows:

$$RA = \frac{N_c}{N_t} \times 100\%$$

where  $N_c$  is the number of steps that were correctly detected;  $N_t$  is the number of total steps. Here, it is worth highlighting that steps during transition strides were not used to calculate RA.

To evaluate the timing of locomotion recognition during mode transitions, we proposed to segment the transition gait into several phases. According to the human locomotion biomechanics defined in [21], [22], the stride cycle in GLW could be segmented into six phases: initial swing (ISW), middle swing (MSW), terminal swing(TSW), initial stance (IST), middle stance (MST), and late stance (LST); the stride cycle in SA could be broken into five gait phases: weight acceptance (WA), pull up (PU), forward continuance (FCN), foot clearance (FCL), and foot placement (FP); the stride cycle in SD could be segmented into 5 phases as well: weight acceptance (WA), forward continuance (FCN), controlled lowering (CL), leg pull-through (LP), and foot placement (FP). Based on the above gait segmentation rules, we defined the locomotion transition gait phases of the leading limb as follows:

- transition from GLW to SA was broken into ISW, MSW, FCL, and FP;
- transition from GLW to SD was broken into ISW, MSW, LP, FP;
- transition from SA to GLW was broken into FCL, MSW, TSW;

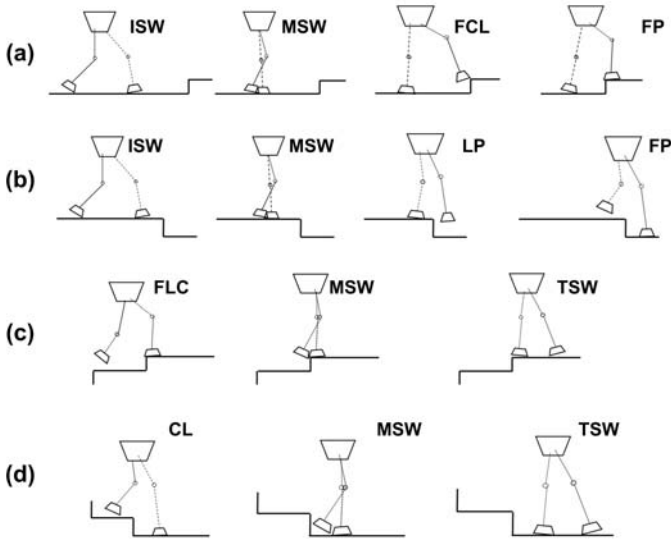


Fig. 6. Sketch view of the segmented gait phases during locomotion mode transition. The solid line indicates the leading limb while the dashed line indicates the lagging limb. These gait phases correspond to transitions: (a) from GLW to SA, (b) from GLW to SD, (c) from SA to GLW, (d) from SD to GLW.

- transition from SD to GLW was broken into CL, MSW, TSW.

A sketch view of these transition gait phases was drawn in Fig. 6. If a transition was detected before the foot lift of the leading limb, it was tagged as one-step early (OSE). If a transition was detected after the foot placement or heel strike of the leading limb, it was tagged as one-step delay (OSD). The OSE and OSD steps were not used to calculate RA during steady state.

All true gait phases and locomotion mode were obtained through referring to the recorded depth images.

#### IV. RESULTS AND DISCUSSION

The average depth values during different locomotion modes were illustrated in Fig. 7(a). A focused view on the depth value variations during task transitions was displayed in Fig. 7(b). It could be found that the average depth values in Block(1,2) and Block(1,3) were clearly differentiated among dynamic locomotion modes, i.e. GLW, SA, and SD. When the subject was in SS, the standard deviations of depth values in Block(3,2), Block(3,3), Block(2,2), and Block(2,3) were around zero, while reaching a much greater value in dynamic modes. Recognition results showed that the SS mode could always be accurately recognized when the subjects stood still. When subjects started moving from SS, the GLW was always detected when the leading limb started moving.

The accuracy and transition timing of the proposed locomotion recognition system were listed in TABLE II. Despite of high variability among the nine subjects, during the steady state, i.e. except transition strides, the RA of GLW, SA, and SD was 100% except for the SA of Subject #5. One

SA step of Subject #5 was detected to be GLW due to the viewed angle of the stair  $\theta$  was smaller than 65 degree. This kind of wrong detection could be corrected by measuring the orientation of the camera, for instance, based on an gyroscope sensor.

According the human locomotion biomechanics [21], [22], the latest transition gait phase should happen at MSW. After MSW, the kinematics and dynamics of both limbs were adapted to the coming new locomotion mode. Taking the transition from GLW to SA as an example, the hip and knee joint angles of the leading limb were much greater in FLC of SA than TSW of GLW while the lagging limb would provide a higher supporting force for the FP of SA than for the heel strike of GLW. According to the transition phases shown in TABLE II, all the transitions were detected during or before the foot placement of the leading limb, i.e. there was no OSD detection. Furthermore, out of the 216 transitions, 82.4% of detections happened no later than the critical transition gait phase, i.e. MSW. These results confirmed that the mode recognition timing of the proposed system was superior compared with classical locomotion detection method based on ground reaction force or mechanical inertia sensors [23], [24], [14]. The later method usually recognizes the transition at the foot placement of the leading limb or with one-step delay.

Among all the locomotion transitions of SA-GLW and SD-GLW, more than 75% of detections were tagged with OSE. This meant that the GLW was triggered when the first limb contacted the ground. At this moment, the trailing limb was in FCN phase, which should have been in LST phase if it was a true GLW transition. Thus, whether a transition was triggered with OSE could be figured out by referring to the posture of the trailing limb. The limb's posture can be captured by means of inertia sensors. Similar strategies could be applied to detect an OSE during transitions of GLW-SA and GLW-SD. Once a transition detection was confirmed to be OSE, the triggering signal could be utilized to predict the true transition, which was expected to happen when the trailing limb reach MSW phase.

Despite the promising prediction performance in transitions of GLW-SD, SA-GLW, and SD-GLW, half transitions of GLW-SA were detected after MSW. By referring to the raw depth images, we found that when the leading limb was lifted to a relatively high position at the end of MSW, the limb would cover the stair line. Without an effective stair edge detection within the predefined dynamic sliding window (Subsection II-C), SA would not be triggered. In the future work, a time-of-flight (ToF) camera could be utilized, which could provide larger range of view with higher sampling rate than the Xtion PRO LIVE camera used in this study.

As a result of the placement strategy of the depth camera (Fig. 1), the depth blocks of the third row would only capture the limb movements. Along with the cyclic movements of the two limbs, the average depth values of these blocks change periodically. In Fig. 7(a), Block(3,1) and Block(3,4) demonstrated a stable periodicity during all dynamic locomotion tasks. This periodic feature offers us an opportunity

TABLE II  
THE RECOGNITION ACCURACY DURING STEADY STATE AND THE GAIT PHASES AT LOCOMOTION TRANSITIONS.

Subject	GLW			SA			SD			GLW-SA			GLW-SD			SA-GLW			SD-GLW		
	$N_t$	RA[%]	$N_t$	RA[%]	$N_t$	RA[%]	No.	Phase	No.	Phase	No.	Phase	No.	Phase	No.	Phase	No.	Phase	No.	Phase	
#1	265	100	66	100	66	100	6	1 ISW, 2 MSW, 3 FCL	6	3 IWS,2 MSW, 1 LP	6	4 MSW,2 TSW	6	5 OSE, 1 MSW							
#2	265	100	66	100	66	100	6	1 OSE,1 ISW,2 MSW,2 FCL	6	6 OSE	6	6 OSE	6	6 OSE							
#3	260	100	66	100	66	100	6	1 ISW, 2 MSW, 3 FCL	6	6 OSE	6	4 OSE,2 FCL	6	6 OSE							
#4	247	100	66	100	66	100	6	2 MSW, 4 FCL	6	3 OSE,1 MSW, 2 LP	6	5 OSE, 1 FCL	6	4 OSE, 2 CL							
#5	228	100	66	98.5	66	100	6	4 FCL, 2 FP	6	4 OSE,2 MSW	6	6 OSE	6	6 OSE							
#6	249	100	66	100	66	100	6	1 ISW, 2 MSW, 3 FCL	6	6 OSE	6	6 OSE	6	2 OSE, 3 CL, 1 MSW							
#7	268	100	66	100	66	100	6	1 MSW, 3 FCL, 2 FP	6	2 OSE, 2 IWS, 1 MSW, 1 LP	6	6 OSE	6	5 OSE, 1 CL							
#8	207	100	66	100	66	100	6	1 MSW, 3 FCL, 2 FP	6	2 OSE, 2 IWS, 1 MSW, 1 LP	6	6 OSE	6	5 OSE, 1 CL							
#9	244	100	66	100	66	100	6	4 ISW, 2 MSW	6	6 OSE	6	2 OSE, 4 FLC	6	4 OSE, 2 CL							
All	2233	100	594	99.8	594	100	54	1 OSE, 8 ISW, 14 MSW 25 FCL, 6 FP	54	35 OSE, 7 IWS 7 MSW, 5 LP	54	41 OSE, 7 FCL	54	43 OSE, 9 CL, 2 MSW							

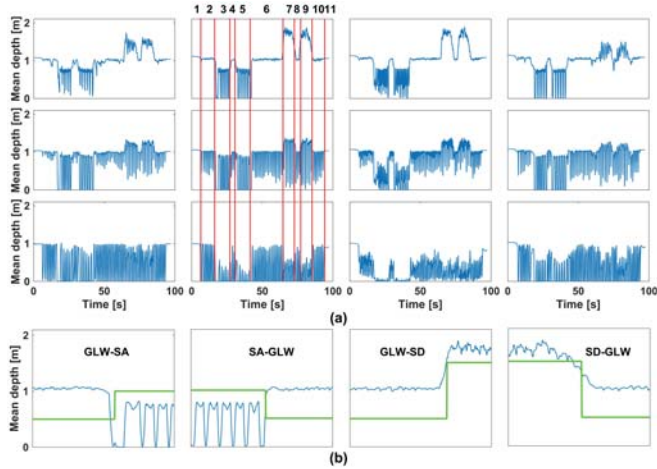


Fig. 7. Example of the average depth values during one track trial. The data was taken from one subject. (a) The average depth values of each image block. The red vertical lines separated the trial into the following tasks: 1 SS, 2 GLW, 3 SA, 4 GLW, 5 SA, 6 GLW, 7 SD, 8 GLW, 9 SD, 10 GLW, 11 SS. (2) A detailed view of the depth values during locomotion mode transitions, which was taken from Block(1,2). The green line marked the transition moments detected by the proposed algorithm.

to estimate the gait frequency and gait phase, which could be further utilized to improve the accuracy of locomotion detection.

A major limitation of this study lies on the absence of a real-time evaluation. In fact, the computation workload of the detection algorithm is quite low. The average time to process one depth image is about 5 ms with MATLAB R2016a running on Intel(R)Core(TM)i7-7820HQ CPU, 2.90 Hz. Therefore, the algorithm can be easily transferred to a real-time system thus detecting the locomotion mode online.

## V. CONCLUSIONS

In this work, a depth image-based environment-aware system has been developed for locomotion mode recognition. The system consists of two subsystems: a depth feature extraction subsystem and a finite-state-machine based locomotion recognition subsystem. Nine healthy young subjects participated in the validation experiments and each of them was asked to perform a continuous locomotion track three times at normal speed. During the experiments, four locomotion modes, including SS, GLW, SA, and SD, and six locomotion transition conditions, including SS-GLW, GLW-SS, GLW-SA, SA-GLW, GLW-SD, and SD-GLW, were analyzed.

An approximate 100% RA was reported for steady state locomotion tasks. Among the 216 mode transitions, 82.4% of the intended locomotion task could be detected before the transition happened, which outperforms most methods in the current literature. The promising results are expected to significantly improve the decision making regarding locomotion transitions of lower-limb wearable robots. Thus, a seamless and smooth assistance could be ensured when the users change their locomotion tasks. In the future work, we will firstly evaluate the performance of the proposed method in real time, which is expected to run smoothly due to the low computation workload. Then, we will validate the locomotion recognition system with elderly subjects who have very different gait patterns. Finally, the system will be tested with a lower-limb exoskeleton system and in an ecological environment.

## ACKNOWLEDGMENT

This work is partially supported by RGC GRF grant # 14205914, ITC ITF grant ITS/236/15, and Shenzhen Science and Technology Innovation project c.02.17.00601 awarded to Prof. Max Q.-H. Meng.

## REFERENCES

- [1] A. M. Dollar and H. Herr, "Lower extremity exoskeletons and active orthoses: challenges and state-of-the-art," *IEEE Transactions on robotics*, vol. 24, no. 1, pp. 144–158, 2008.
- [2] W. Huo, S. Mohammed, J. C. Moreno, and Y. Amirat, "Lower limb wearable robots for assistance and rehabilitation: A state of the art," *IEEE systems Journal*, vol. 10, no. 3, pp. 1068–1081, 2016.
- [3] K. Yoshikawa, M. Mizukami, H. Kawamoto, A. Sano, K. Koseki, Y. Hashizume, Y. Asakawa, K. Iwamoto, Y. Kohno, H. Nagata *et al.*, "Hybrid assistive limb enhances the gait functions in sub-acute stroke stage: A multi single-case study," *Physiotherapy Practice and Research*, vol. 37, no. 2, pp. 91–100, 2016.
- [4] F. Giovacchini, F. Vannetti, M. Fantozzi, M. Cempini, M. Cortese, A. Parri, T. Yan, D. Lefebvre, and N. Vitiello, "A light-weight active orthosis for hip movement assistance," *Robotics and Autonomous Systems*, vol. 73, pp. 123–134, 2015.
- [5] F. A. Panizzolo, I. Galiana, A. T. Asbeck, C. Siviy, K. Schmidt, K. G. Holt, and C. J. Walsh, "A biologically-inspired multi-joint soft exosuit that can reduce the energy cost of loaded walking," *Journal of neuroengineering and rehabilitation*, vol. 13, no. 1, p. 43, 2016.
- [6] S. Wang, L. Wang, C. Meijneke, E. Van Asseldonk, T. Hoellinger, G. Cheron, Y. Ivanenko, V. La Scaleia, F. Sylos-Labini, M. Molinari *et al.*, "Design and control of the mindwalker exoskeleton," *IEEE transactions on neural systems and rehabilitation engineering*, vol. 23, no. 2, pp. 277–286, 2015.
- [7] S. Au, M. Berniker, and H. Herr, "Powered ankle-foot prosthesis to assist level-ground and stair-descent gaits," *Neural Networks*, vol. 21, no. 4, pp. 654–666, 2008.
- [8] J. L. Pons, *Wearable robots: biomechatronic exoskeletons*. John Wiley & Sons, 2008.

- [9] T. Yan, M. Cempini, C. M. Oddo, and N. Vitiello, "Review of assistive strategies in powered lower-limb orthoses and exoskeletons," *Robotics and Autonomous Systems*, vol. 64, pp. 120–136, 2015.
- [10] D. Novak and R. Riener, "A survey of sensor fusion methods in wearable robotics," *Robotics and Autonomous Systems*, vol. 73, pp. 155–170, 2015.
- [11] H. Huang, F. Zhang, L. J. Hargrove, Z. Dou, D. R. Rogers, and K. B. Englehart, "Continuous locomotion-mode identification for prosthetic legs based on neuromuscular-mechanical fusion," *IEEE Transactions on Biomedical Engineering*, vol. 58, no. 10, pp. 2867–2875, 2011.
- [12] M. Mathie, B. G. Celler, N. H. Lovell, and A. Coster, "Classification of basic daily movements using a triaxial accelerometer," *Medical and Biological Engineering and Computing*, vol. 42, no. 5, pp. 679–687, 2004.
- [13] B. Coley, B. Najafi, A. Paraschiv-Ionescu, and K. Aminian, "Stair climbing detection during daily physical activity using a miniature gyroscope," *Gait & posture*, vol. 22, no. 4, pp. 287–294, 2005.
- [14] K. Yuan, A. Parri, T. Yan, L. Wang, M. Munih, N. Vitiello, and Q. Wang, "Fuzzy-logic-based hybrid locomotion mode classification for an active pelvis orthosis: Preliminary results," in *Engineering in Medicine and Biology Society (EMBC), 2015 37th Annual International Conference of the IEEE*. IEEE, 2015, pp. 3893–3896.
- [15] A. Parri, E. Martini, J. Geeroms, L. Flynn, G. Pasquini, S. Crea, R. M. Lova, D. Lefeber, R. Kamnik, M. Munih *et al.*, "Whole body awareness for controlling a robotic transfemoral prosthesis," *Frontiers in neurorobotics*, vol. 11, 2017.
- [16] M. Liu, D. Wang, and H. H. Huang, "Development of an environment-aware locomotion mode recognition system for powered lower limb prostheses," *IEEE Transactions on Neural Systems and Rehabilitation Engineering*, vol. 24, no. 4, pp. 434–443, 2016.
- [17] N. E. Krausz, T. Lenzi, and L. J. Hargrove, "Depth sensing for improved control of lower limb prostheses," *IEEE Transactions on Biomedical Engineering*, vol. 62, no. 11, pp. 2576–2587, 2015.
- [18] H. A. Varol and Y. Massalin, "A feasibility study of depth image based intent recognition for lower limb prostheses," in *Engineering in Medicine and Biology Society (EMBC), 2016 IEEE 38th Annual International Conference of the IEEE*. IEEE, 2016, pp. 5055–5058.
- [19] T. M. Owings and M. D. Grabiner, "Variability of step kinematics in young and older adults," *Gait & posture*, vol. 20, no. 1, pp. 26–29, 2004.
- [20] R. O. Duda and P. E. Hart, "Use of the hough transformation to detect lines and curves in pictures," *Communications of the ACM*, vol. 15, no. 1, pp. 11–15, 1972.
- [21] D. A. Winter, *Biomechanics and motor control of human movement*. John Wiley & Sons, 2009.
- [22] B. J. McFadyen and D. A. Winter, "An integrated biomechanical analysis of normal stair ascent and descent," *Journal of biomechanics*, vol. 21, no. 9, pp. 733–744, 1988.
- [23] P. C. Formento, R. Acevedo, S. Ghoussayni, and D. Ewins, "Gait event detection during stair walking using a rate gyroscope," *Sensors*, vol. 14, no. 3, pp. 5470–5485, 2014.
- [24] M. Sekine, T. Tamura, T. Fujimoto, and Y. Fukui, "Classification of walking pattern using acceleration waveform in elderly people," in *Engineering in Medicine and Biology Society, 2000. Proceedings of the 22nd Annual International Conference of the IEEE*, vol. 2. IEEE, 2000, pp. 1356–1359.